CHAPTER II

UP-REGULATION OF ANNEXIN A2 IN CHOLANGIOCARCINOMA CAUSE BY OPISTHORCHIS VIVERRINI AND ITS IMPLICATION AS A PROGNOSTIC MARKER

2.1 Introduction

Cholangiocarcinoma (CCA) is a primary cancer of the bile ducts. In Thailand, the highest incidence of CCA is found in the northeastern region and is primarily associated with the liver fluke *Opisthorchis viverrini* infection. *O. viverrini* is a food-borne trematode which chronically infects the bile ducts of human beings. People become infected by eating raw or undercooked freshwater fish in dishes such as koi pla which contain the fluke metacercaria. Immature flukes migrate up through the ampulla of Vater to the biliary tree and mature in the small intrahepatic ducts (Sripa et al., 2008). An estimated 6 million people are infected with *O. viverrini* in Thailand. The geographical pattern of liver fluke infection is not uniform, however, with the greatest prevalence in the north (19.3%) and northeast (15.7%) compared with the central (3.8%) and southern regions (0%). Despite wide-spread treatment with praziquantel, the prevalence of *O. viverrini* in some endemic areas approaches 70% (Jongsuksuntigul et al., 2003). It has long been known that infection with *O. viverrini* is associated with the induction of CCA (Sriamporn et al., 2004; Sriamporn et al., 2005; Sripa et al., 2007), indeed there is no stronger link between an eukaryotic organism and a malignant neoplasm than that between *O. viverrini* and CCA. This has led the World Health Orgainization's International Agency for Research on Cancer to classify *O. viverrini* as a Group 1 carcinogen to humans (Bouvard et al., 2009). For unknown reasons, cases of CCA are increasing worldwide (Blechacz et al., 2008). Only the surgical resection of all detectable tumors leads to an improvement in the 5-year survival rate. However, a complete resection is often impossible, typically resulting in subsequent metastasis and local recurrence (Olnes et al., 2004). At present, there are no specific tumor markers that can indicate the early stages and

status of CCA. Thus, there is a need for tumor markers that can be measured early and in easily accessible samples such as plasma.

Mass spectrometry (MS) is a powerful approach for the identification of differentially expressed, low-abundance proteins that may be useful as tumor markers. Proteomic approaches have been successfully employed in studies of breast (Kischel et al., 2008) and prostate (Sardana et al., 2007) cancers for tumor marker discovery. Of particular interest in these studies are the proteins expressed on the surface of tumor cells and characterization of cell surface proteomes could provide a better understanding of the manner in which those are regulated. However, proteome-wide analysis of surface membrane proteins has thus far been hampered by the lack of effective strategies to profile hydrophobic membrane proteins. A method to overcome this problem, sequential protein extraction combined with Tris, DTT and Tributylphosphine (TBP), has recently been utilized to isolate and identify surface proteins from human breast cancer cell lines (Ruan et al., 2007). In the present work, we interrogated the cell membranes of human CCA cell lines using two-dimensional gel electrophoresis (2-DE) in order to identify proteins associated with the plasma membrane, and to understand the cellular abundance and status of these proteins. This has allowed us to detect tumor markers for CCA, with one protein of particular interest, annexin A2 (ANXA2), identified by MALDI-TOF MS. Over-expression of ANXA2 has been directly implicated in liver cancer progression (Mohammad et al., 2008; Ji et al., 2009), and here we show its utility as a potential prognostic marker for *O. viverrini*-induced CCA.

2.2 Materials and Methods

2.2.1 Cell cultures

Four human CCA cell lines, namely KKU-M156 (M156), KKU-100 (K100), KKU-139 (M139) and KKU-M213 (M213), were isolated from CCA patients from northeastern Thailand. Cell lines were developed and cultured as described elsewhere (Sripa et al., 2005). In all cases, CCA was linked to infection with *O. viverrini*. Approval for use of the tissue was obtained from the Human Research Ethics Committee of Khon Kaen University, Thailand. CCA tissues were histologically characterized based on their marginal zones as moderately

differentiated adenocarcinoma (M156), poorly differentiated adenocarcinoma (K100), squamous cell carcinoma (M139) and adenosquamous cell carcinoma (M213). CCA cell lines were cultured in RPMI-1640 medium (Gibco, Grand Island, NY, USA) containing 100 U/ml penicillin and 100 μg/ml streptomycin with 10% FBS (Hyclone Laboratories). H69 cells, a human 'immortalized', non-malignant cholangiocyte cell line, were cultured as previously described (Grubman et al., 1994). Cell growth was performed at 37 °C under 5% CO_2 and 95% humidified air. During this experiment mycoplasma contamination was periodically checked and no contamination was present in any cell line.

2.2.2 Clinical tissue samples

In this study, CCA tissues were obtained with informed consent from the patients who underwent hepatectomy at Srinagarind hospital, Khon Kaen University, Thailand. The experimental protocol was approved by the Human Research Ethics committee of Khon Kaen University (IRB number HE42075). All tumors were clinically and histologically diagnosed as intrahepatic CCA (ICC) according to WHO classifications (Nakanuma et al., 2000). Patient information was obtained from medical records. Infection with *O. viverrini* in the patients was diagnosed as positive if the patient fulfilled one of these four criteria: (i) a history of previous positive stool examination for *O. viverrini* or its eggs; (ii) identification of *O. viverrini* or its eggs in stool or bile; (iii) demonstration of a typical bead-like cholangiogram; or (iv) histological evidence of *O. viverrini* in the specimen (Watanapa, 1996). Of the 301 liver fluke-associated CCA patients explored, 203 were male and 98 were female with a male to female ratio of 2:1. The mean age was 55 ± 9 years (range, 31-75 years). Most of the patients were at an advanced CCA stage, with 73.9% lymphatic, 53.1% vascular and 39.6% neural invasion. Thirty-five percent of the tumors had well-differentiated histopathological grading. The majority of patients (63.5%) possessed a tumor size > 5 cm.

2.2.3 Sample preparation

Cells were examined under a phase-contrast microscope to ensure that they were 90–95% confluent before lysis. The culture medium was discarded and the cells were washed with 0.25 M sucrose three times on ice. Cells were scraped thoroughly with a scraper in 0.25 M sucrose containing 1% Protease Inhibitor Mix

(Amersham Biosciences). The cells were collected and centrifuged at 1,500 x*g* at 4 °C for 5 min. The pellets were resuspended in lysis buffer containing 7 M urea, 2 M thiourea, 4% CHAPS (zwitterionic detergent commonly used in isoelectric focusion; IEF), 2% immobilized pH gradient (IPG) buffer 3-10 NL, 40 mM DTT, and 1% Protease Inhibitor Mix and allowed to lyse on ice for 15 min. Cell lysates were sonicated according to the manufacturer's instructions (Sonics & Materials Inc. VCX 400, USA) and incubated at 4 °C for 2 h. The lysate was then centrifuged at 600 x*g* for 10 min to remove the nuclei and unlysed cells. The supernatant was centrifuged at 17,000 x*g* for 30 min to harvest crude membrane fractions, then washed twice in ice-cold 0.25 M sucrose and centrifuged at 17,000 x*g* for another 30 min. The membrane-enriched fractions were then resuspended in extraction buffer (7 M urea, 2 M thiourea, 4% CHAPS, 1% IPG buffer 3-10 NL, 50 mM DTT, 20 mM Tris, 0.5% Triton X-100, and 1% Protease Inhibitor Mix) at 4 °C and were subjected to vortexing every 5 min for 1 h followed by centrifugation at 20,000 x*g* for 1 h. The supernatant was collected and protein concentration was determined by Bradford Assay using a VersaMax™ absorbance microplate reader (Molecular Devices Corporation California, USA) at 595 nm. Membrane proteins of each cell line were then ready for 2-DE.

2.2.4 2-DE and image analysis

2-DE was performed using the Immobiline/polyacrylamide system. For active rehydration loading, the strips were rehydrated with 125 µl rehydration buffer (7 M urea, 2 M thiourea, 4% CHAPS, 0.5% Triton X-100, 0.5% IPG buffer, 5 mM TBP with 30 mM DTT) containing 100 µg protein and applied to 7 cm pH 3-10 NL IPG strips (Amersham Biosciences, Sweden) by in-gel rehydration (20 V, 12 h), after which isoelectric focusing was performed for 17,840 Vh. IPG strips were then incubated in equilibration buffer (50 mM Tris, pH 8.8, 6 M urea, 30% glycerol, 10% SDS with a trace of bromophenol blue) containing 1% DTT for 15 min followed by 15 min incubation in equilibration buffer supplemented with 2.5% iodoacetamide. The IPG strips were then applied to the second-dimensional 12.5% SDS-polyacrylamide gels. Electrophoresis of the mini-gel was performed in a Hoefer system at 20 mA at room temperature for 2 h. The proteins were fixed in the gel and visualized after CBR-250 (GE Healthcare) staining. Stained gels were scanned using

an ImageScanner (Amersham Biosciences, Sweden) and analyzed using ImageMaster™ 2D Platinum 6.0 software (GE Healthcare).

2.2.5 Tryptic in-gel digestion of 2-DE spots, MS analysis and protein identification

Protein spots that were unique to or stained more intensely in CCA cell lines compared with H69 cells were excised from the gel and transferred to V-bottom 96-well microtitre plates. Tryptic digestions were performed on an EttanTM Spot Handling Workstation robot (Amersham Biosciences) according to the manufacturer's specifications. The 10 mg of matrix solution, α-cyano-4-hydroxycinnamic acid (Bruker Daltonik GmbH, Germany), was prepared by dissolving to saturation in 50% acetronitrile/water with 0.1% trifluoroacetic acid and then mixed with equal volumes of tryptic peptides with matrix solution. The mixture (1 μl) was spotted onto a steel target surface (MTP 384 ground steel, Bruker Daltonik) and dried by air. Mass spectra were recorded on an Autoflex MALDI-TOF mass spectrometer (Bruker Daltonik) with delayed extraction, 2GHz LeCroy digitizer and a 337 nm N_2 laser. The MALDI-TOF MS was calibrated using trypsin auto-digestion peptide signals and matrix ion signals. Typically, 100 shots were accumulated from three to five different positions within a sample spot. The mass spectra were analyzed using MALDI evaluation software (Amersham Biosciences). Proteins were identified by peptide mass fingerprinting using Mascot (http://www.matrixscience.com) in searches against the NCBI non-redundant protein database (NCBInr). Parameters used in Mascot searches were as follows: taxonomy was restricted to *Homo sapiens*, trypsin was specified with allowance for one missed cleavage, a 2 Da peptide tolerance was allowed, and carbamidomethyl and oxidized methionine were chosen as the fixed and variable modifications, respectively. A threshold of 5% probability (p-value < 0.05) of a false positive was applied for all Mascot searches.

2.2.6 Western blot analyses

After 2-DE proteins were transferred to nitrocellulose membrane. The membrane was blocked with 5% skimmed milk in PBS/0.05% Tween-20 (PBS-T) for 2 h. The membrane was incubated overnight with mouse anti-Annexin II (SKU 03-4400, Invitrogen) diluted 1:1,000 (v/v) in 2% skimmed milk in PBS-T at 4°C. After washing 3 × 5 min with PBS-T the membrane was incubated in horseradish

peroxidase (HRP)-conjugated goat anti-mouse antibody (Zymed Laboratories) diluted 1:2,000 (v/v) in 2% skimmed milk in PBS-T at 25°C for 1 h. The membrane was washed again for 3 × 5 min with PBS-T followed by a final 10 min rinse with PBS. Reactive spots were visualized with diaminobenzidine (DAB, Sigma Chemical Co).

2.2.7 Tissue microarray and immunohistochemistry

Tissue microarrays (TMAs) were constructed by the Department of Pathology, Faculty of Medicine, Khon Kaen University, Thailand. Following TMA construction (Fedor et al., 2005), an H&E stained section of the TMA recipient block was prepared and reviewed to confirm the presence of intact neoplasm. The arrays contained a total of 301 *O. viverrini*-associated CCA cases. One core was taken from each formalin-fixed, paraffin-embedded CCA sample by using punch cores that measured 0.9 mm in greatest diameter from the non-necrotic area of tumor foci.

Immunohistochemical reactions were performed on 4 μm-thick sections of TMA silane-coated slides (Sigma, St. Louis, MO, USA) by an immunoperoxidase method. TMA sections were deparaffinized in xylene and rehydrated in serial graded ethanol and distilled water, respectively. Antigen retrieval was performed by immersion of tissue sections in pre-heated 10 mM, pH 6.0 citrate buffer and maintaining heat at 120 °C in a pressure cooker for 5 min. Endogenous peroxidase activity was eliminated by treating sectioned tissues with absolute methanol containing 3% H_2O_2 for 30 min. The sections were then washed in water and PBS. Non-specific staining was blocked by treating slides with 5% normal horse serum in PBS for 30 min. The sections were probed with mouse anti-Annexin II (as described earlier) diluted 1:400 (v/v) in PBS and incubated overnight at 4°C. After rinsing for 3 × 5 min with PBS the sections were incubated with HRP-conjugated goat anti-mouse IgG (Abcam Inc., USA) for 1 h. Sections were rinsed with PBS for 2 × 10 min, after which the sections were developed with DAB (Sigma Chemical Co.). The sections were counterstained with Mayer's hematoxylin, dehydrated, cleared in xylene and mounted in Permount.

2.2.8 Assessment of IHC staining and statistical analyses

Immunoreactivity was evaluated independently by three researchers (Ponlapat Yonglitthipagon, Banchob Sripa and Chawalit Pairojkul) who were blinded to patient outcome. Consensus was reached whenever disagreement occurred.

The percentage of positive tumor cells was determined using interactive stereological immunoscoring based on systematic random sampling (van Diest et al., 1997) and the average score was calculated. As show in Figure 2.1, within a defined area of the lesion, we randomly selected five high-power fields (magnification, x400; 100 cells/high-power field) and approximately 500 tumor cells were counted. In this study the percentage of positive cells expressing ANXA2 was categorized: <10% (-), ≥ 10% (+) as described elsewhere (Zhuang et al., 2008). The extent of invasion by the cancer was determined in both tumorous and non-tumorous liver tissues by a senior pathologist (Chawalit Pairojkul). Lymphatic and vascular invasion was detected by the presence of infiltrating cancer cells within the lymphatic or blood vessels, respectively. Neural invasion was presented as positive cancer cells in the perineurium and/or neural fascicle.

Statistical analyses of the data were performed with the SPSS version 16.0 statistical package. For cross-sectional analyses, the chi-square test was utilized to analyze the relation between ANXA2 expression and categorical variables regarding clinical pathology parameters. Patient survival was calculated from the time of surgical resection to either the date of death regardless of cause or the most recent contact. The survivors were censored at the date they were last known to be alive. The Kaplan–Meier method was used to calculate cumulative survival. Deaths from causes other than the index tumor or its metastases were not considered to be treatment failures and were excluded from the final analyses of specific survival for the illness. Differences in survival between ANXA2 (-) and AXNA2 (+) groups were analyzed for significance by the log-rank method. The Cox-regression model was used to perform multivariate analysis and values of $p < 0.05$ were considered statistically significant. A schematic representation of the methods outline is summarized in Figure 2.2.

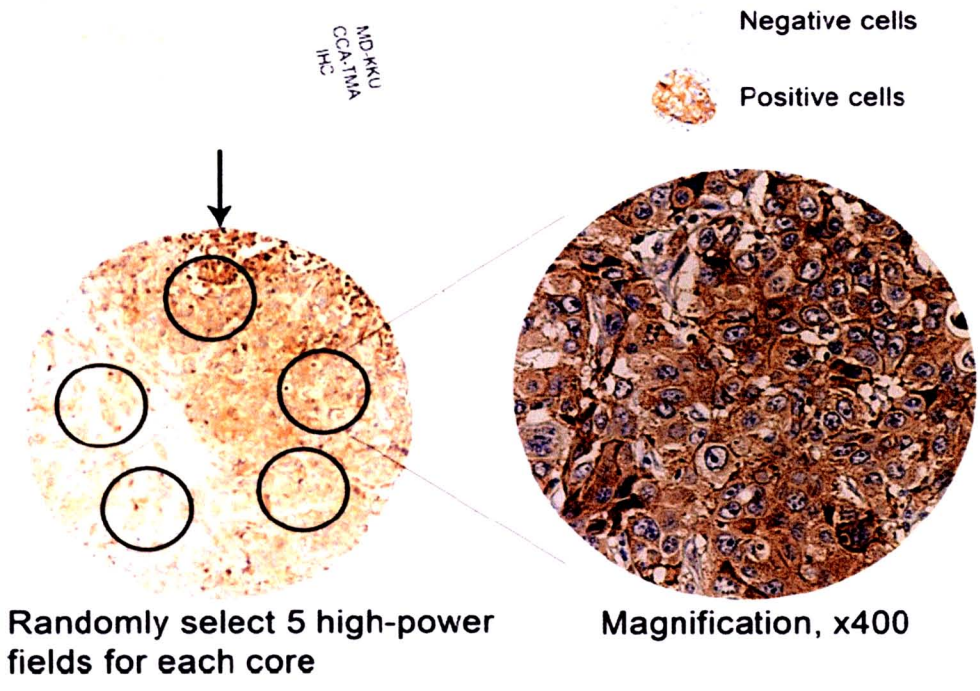

Figure 2.1 Schematic explanation of the protocol for interactive stereological immunoscoring based on systematic random sampling. Within a defined area of each tumor care in tissue microarray (TMA) of human *Opisthorchis viverrini*-associated CCA tissues. Five high-power fields (magnification, 400x; 100 cells/high-power field) were randomly selected and approximately 500 tumor cells were counted.

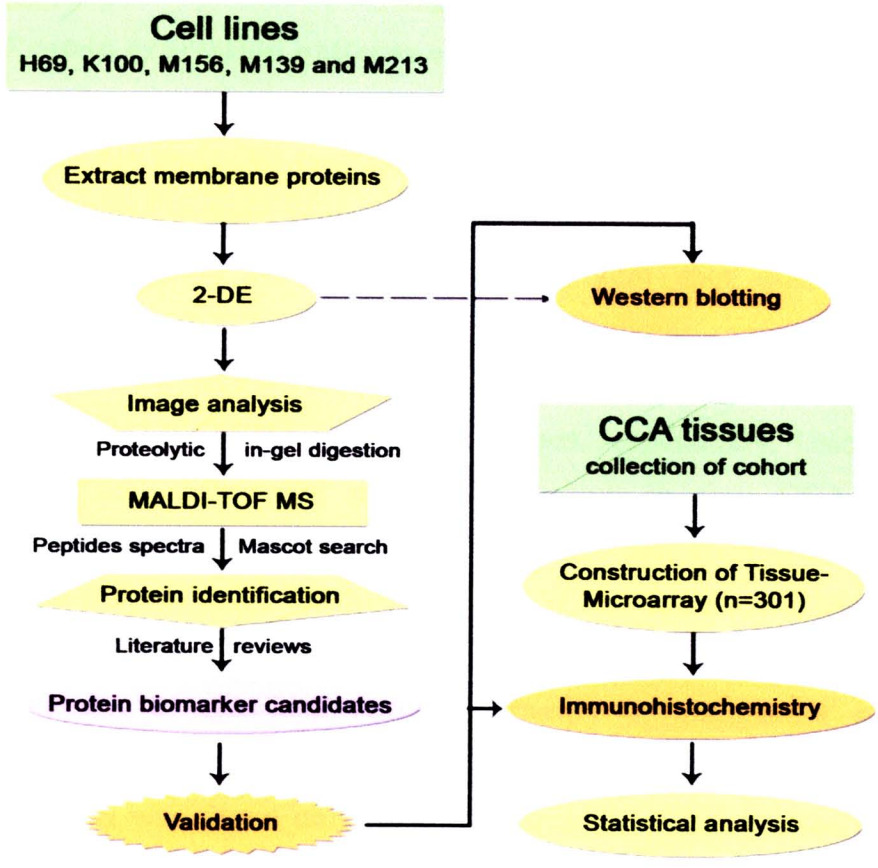

Figure 2.2 Overview of combined proteomics and tissue microarray (TMA) procedures. Membrane proteins were extracted from cholangiocarcinoma (CCA) cell lines and separated by two-dimensional gel electrophoresis (2-DE). After image analysis, gel spots were excised and subjected to in-gel tryptic digestion. Peptides were analyzed by MALDI-TOF-MS. Peptide mass fingerprinting (PMF) spectra were matched to human protein sequences after database searching and identified proteins were selected as potential biomarker candidates according to literature searches. Protein biomarker candidates were validated by Western blotting and immunohistochemistry to confirm the expression and the distribution of these proteins. The TMA of human *Opisthorchis viverrini*-associated CCA tissues was applied to provide a high-throughput validation of potential targets identification in the proteomics study.

THE NATIONAL RESEARCH COUNCIL OF THAILAND
RESEARCH LIBRARY

2.3 Results

2.3.1 Protein expression patterns of CCA cell lines

In order to examine the differential protein profiles of CCA cell lines, three replicate maps for each cell type (M156, K100, M139, M213 and H69) were generated. The separated protein spots were visualised on 2-DE gels by CBR-250 staining, which allows good reproducibility and protein spot quantification for comparative analysis. The 2-DE gel containing the membrane proteins (Figure 2.3) showed a total of 186 ± 20, 314 ± 93, 320 ± 17, 210 ± 35, and 270 ± 6 protein spots, for the M156, K100, M139, M213 and H69 cell lines, respectively. Using 2DE gel replicates, identical and differential protein expression in four CCA cell lines subtracted from H69 were measured. In Table 2.1, the proteins corresponding to spots that were expressed only in CCA cell lines but not in H69 are shown, together with the MS identification parameters. In the tumor histology comparison, mitochondrial ATP synthase, keratin 8, aldo-keto reductase family 1, manganese superoxide dismutase (MnSOD) and heat shock protein 70 (Hsp70) were found only in K100 versus keratin 7 which was found only in M156. Splicing factor proline/glutamine-rich and calreticulin were expressed in M139 whereas the epithelial cell marker protein 1, enolase 1 and tubulin-beta were observed only in M213. We found the solute carrier family 25 protein (SLC25) was expressed in all CCA cell lines as were tubulin-alpha and keratin 18, except the latter was not expressed in M156. The Tu translation elongation factor and keratin 17 were found in the CCA cell lines except for K100. Glycerealdehyde-3 phosphate dehydrogenase, ANXA2, and keratin 19 were found in M213 and M139 compared with chaperonin-containing TCP1 found only in M139 and M156. Although SLC25 was found in all CCA cell lines, the *aberrant* protein expression of SLC25 has not been reported to be associated with any human tumors to date. In contrast, ANXA2 has been reported to play a key role in tumor invasion and metastasis in multiple neoplasms (Bao et al., 2009; Braden et al., 2009; Nedjadi et al., 2009; Zhang et al., 2009) but has not yet been reported as being up-regulated in CCA. Accordingly, in this study, we selected ANXA2 for further verification using Western blots for membrane proteins from M139 and IHC for CCA tissues on the TMA (n = 301).

The National Research Council of Thailand
Research Library
Date 1 2 ก.ค. 2555
Record No. E41042
Call No.

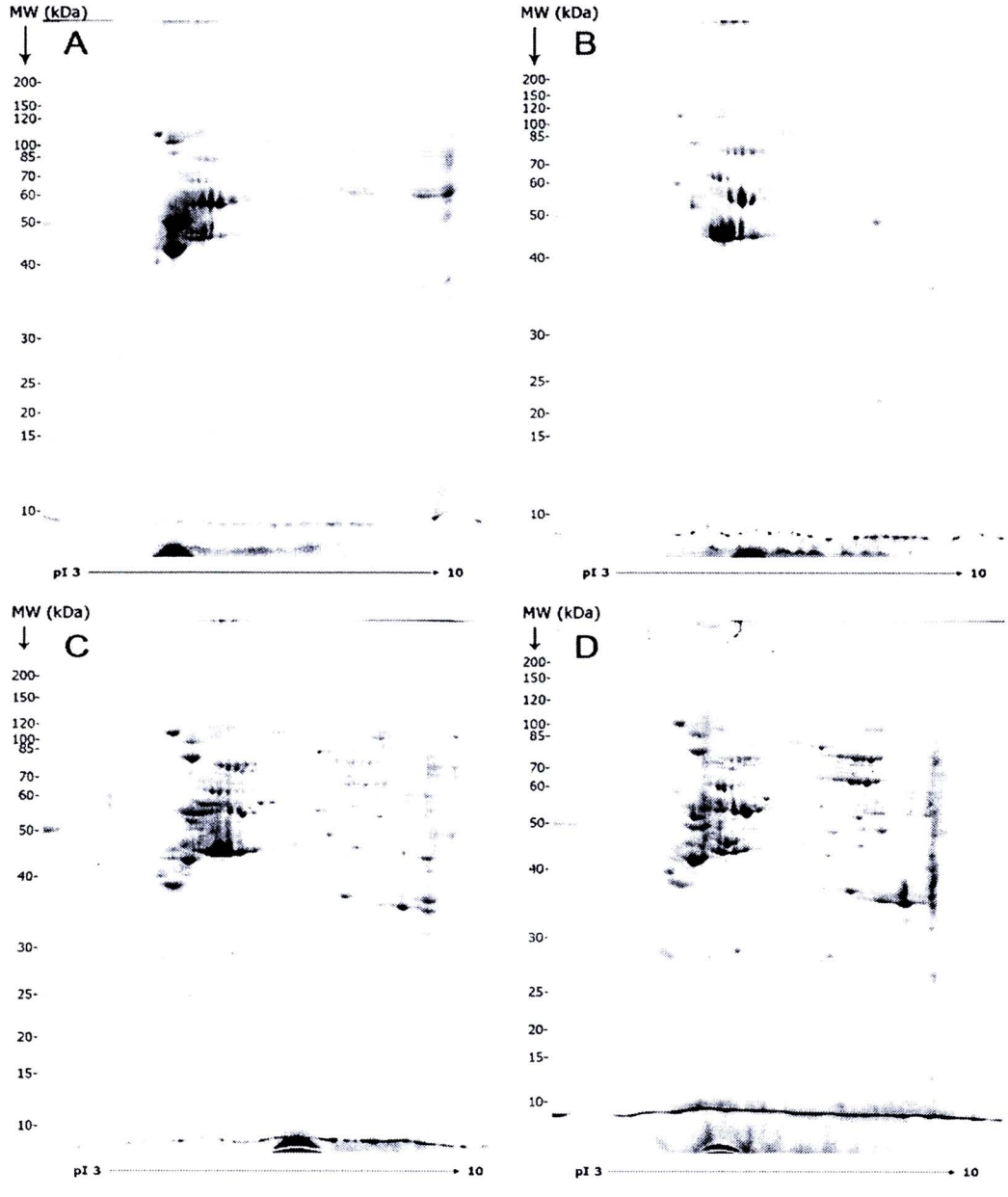

Figure 2.3 Displayed membrane protein profiles of *Opisthorchis viverrini* induced cholangiocarcinoma (CCA) cell lines identified by 2-DE. M156 moderately differentiated CCA (A), K100 poorly differentiated CCA (B), M139 squamous cell carcinoma (C) and M213 adenosquamous cell carcinoma (D). IPG strip of 7 cm, pH 3–10 nonlinear gradient was used in the first dimension and 12.5% SDS-PAGE was used in the second dimension. The protein loading was 100 μg and the gel was stained with CBR-250.

Table 2.1 Membrane proteins differentially expressed in *Opisthorchis viverrini*-induced cholangiocarcinoma (CCA) cell lines identified by MALDI-TOF MS.

Accession No.	MS	CO	M/UM	Description	*Mr*	p*I*	*Normal cell line*	CCA cell lines			
							H69	M156	K100	M139	M213
gi|46249805	96	23	10/12	Solute carrier family 25	53.5	6.0	-	+	+	+	+
gi|109096498	230	61	17/16	Tubulin, alpha	53.5	4.9	-	-	+	+	+
gi|4557888	101	40	14/22	Keratin 18	48.0	5.3	-	-	+	+	+
gi|4557701	454	73	35/15	Keratin 17	48.4	5.0	-	+	-	+	+
gi|34147630	328	61	27/6	Tu translation elongation factor	53.5	7.3	-	+	-	+	+
gi|7669492	155	38	11/8	Glyceraldehyde-3-phosphate dehydrogenase	36.2	8.6	-	-	-	+	+
gi|4757756	235	64	19/12	Annexin A2 isoform 2	38.8	7.6	-	-	-	+	+
gi|24234699	336	63	26/9	Keratin 19	44.1	5.0	-	-	-	+	+
gi|5453603	129	31	13/15	Chaperonin containing TCP1, subunit 2	57.8	6.0	-	+	-	+	-
gi|67782365	322	55	27/10	Keratin 7	51.4	5.4	-	+	-	-	-
gi|89574029	102	66	27/18	Mitochondrial ATP synthase	48.1	5.0	-	-	+	-	-
gi|24234688	128	52	31/9	Heat shock 70	73.9	5.9	-	-	+	-	-
gi|4504919	364	57	34/10	Keratin 8	53.7	5.5	-	-	+	-	-
gi|4502049	193	41	15/7	Aldo-keto reductase family 1	36.2	6.5	-	-	+	-	-
gi|14488599	162	45	12/26	Manganese Superoxide Dismutase	22.2	6.9	-	-	+	-	-
gi|119627826	150	40	18/12	Splicing factor proline/glutamine-rich	66.4	9.2	-	-	-	+	-
gi|62897681	172	41	18/26	Calreticulin	47.1	4.3	-	-	-	+	-
gi|187302	319	77	23/26	Epithelial cell marker protein 1	27.9	4.7	-	-	-	-	+
gi|4503571	156	66	24/4	Enolase 1	47.5	7.0	-	-	-	-	+
gi|57209813	191	36	23/12	Tubulin, beta polypeptide	48.1	4.7	-	-	-	-	+

Note: The presence of a protein in the relevant study is denoted with a '+' and the absence with a '-'. MS, Mowse score ($p < 0.05$); CO, percentage of sequence coverage; M/UM, the number of matched peaks/unmatched peaks.

2.3.2 Western blotting and MS

Membrane proteins from M139 cells were separated by 2-DE and electro-blotted onto nitrocellulose membrane to be probed with commercially available ANXA2 antibody. Fig. 2.4A shows the corresponding CBR-250-stained gel. Figure 2.4B shows the image obtained from analyzing M139 membrane proteins by 2-D immunoblotting with anti-ANXA2 antibody. Three different electrophoretic spots proved to be immunoreactive in the experimental window reported (pH 3–10, mass 10–200 kDa) showing approximately the same M_r, but different p*I* values. The presence of protein variants differing in charge through amino acid differences or post-translational modifications is the most straightforward explanation of these shifts (Pastorelli et al., 2007). Representative mass spectra and the sequences of the assigned peptides for ANXA2 isoform 2 are shown in Figure 2.5.

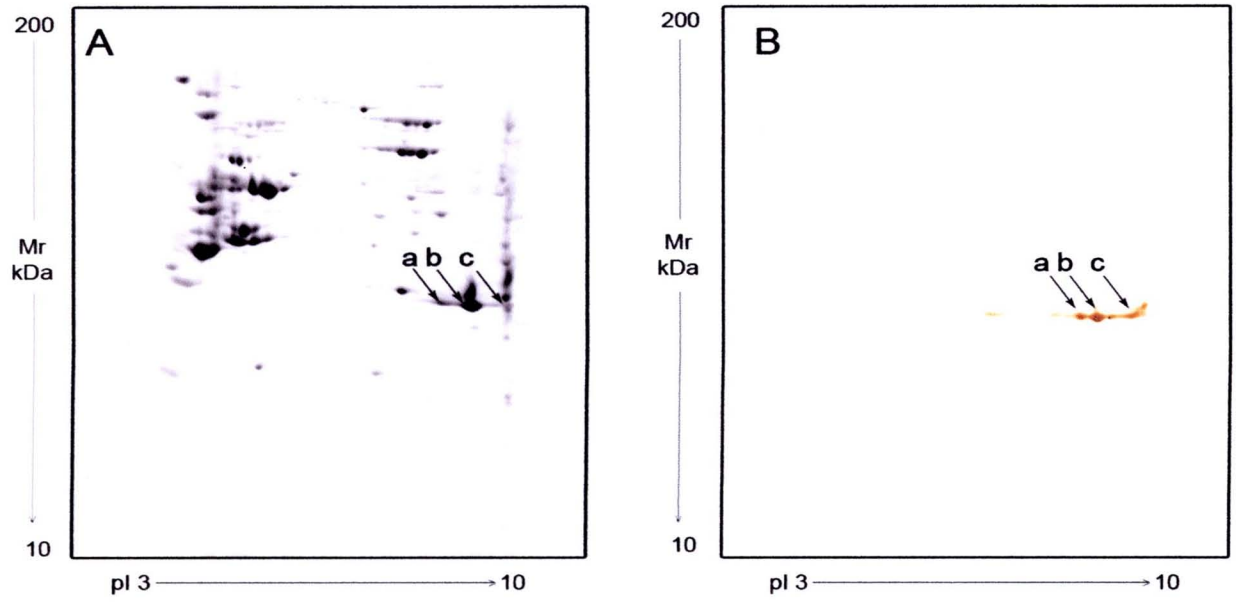

Figure 2.4 Western blot analysis of ANXA2 in two-dimensional electrophoresed gel of purified membrane proteins from M139, *Opisthorchis viverrini* induced cholangiocarcinoma cell line (A). Two-dimensional immunoblotting with anti-Annexin A2 (ANXA2) antibody (B). Three immunoreactive spots are indicated (spot a: 38.8 kDa, p*I* 7.57; spot b: 38.8 kDa, p*I* 7.6; spot c: 38.8 kDa, p*I* 7.65).

A

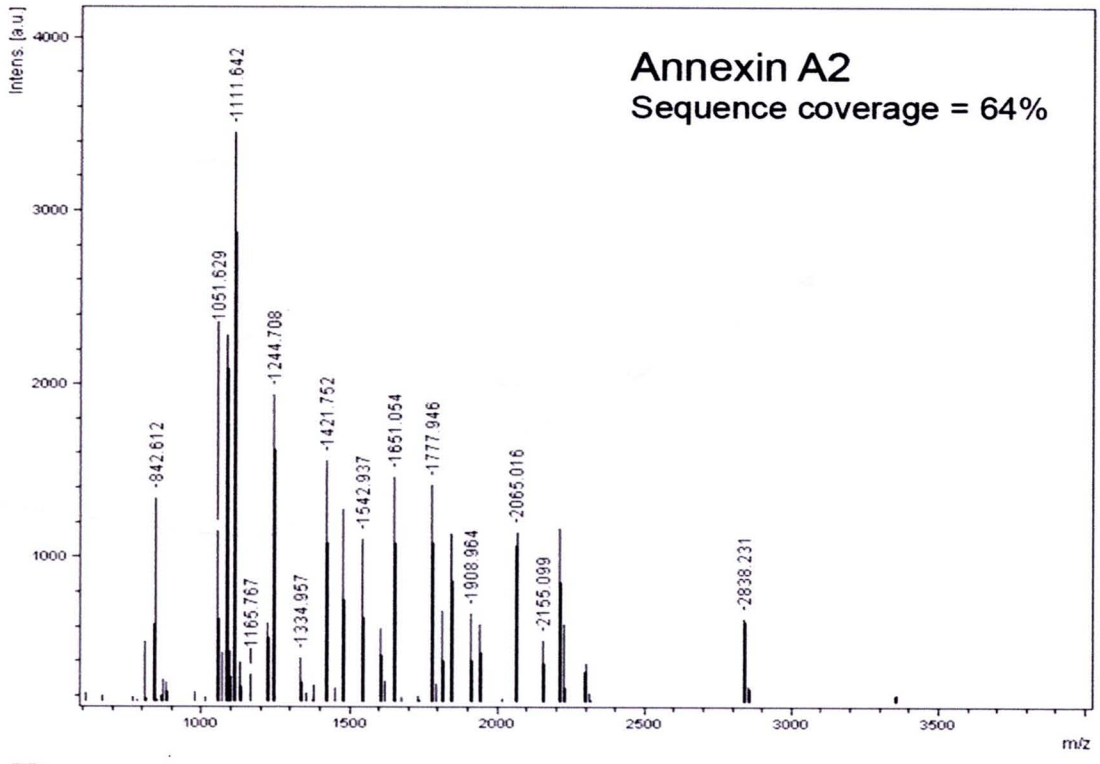

B

```
  1 MSTVHEILCK  LSLEGDHSTP  PSAYGSVKAY  TNFDAERDAL  NIETAIKTKG
 51 VDEVTIVNIL  TNRSNAQRQD  IAFAYQRRTK  KELASALKSA  LSGHLETVIL
101 GLLKTPAQYD  ASELKASMKG  LGTDEDSLIE  IICSRTNQEL  QEINRVYKEM
151 YKTDLEKDII  SDTSGDFRKL  MVALAKGRRA  EDGSVIDYEL  IDQDARDLYD
201 AGVKRKGTDV  PKWISIMTER  SVPHLQKVFD  RYKSYSPYDM  LESIRKEVKG
251 DLENAFLNLV  QCIQNKPLYF  ADRLYDSMKG  KGTRDKVLIR  IMVSRSEVDM
301 LKIRSEFKRK  YGKSLYYYIQ  QDTKGDYQKA  LLYLCGGDD
```

Figure 2.5 MALDI-TOF peptide mass fingerprint of the tryptic digest of annexin A2 (ANXA2). The MALDI-TOF mass spectrum of ANXA2, yielding 64% protein sequence coverage (A) and the matched peptide sequences were underlined (B).

2.3.3 Expression of ANXA2 and clinicopathological findings

IHC analyses were carried out on the TMAs (n = 301) to determine whether ANXA2 expression changes during cholangiocarcinogenesis. Hyperplastic bile duct (Figure 2.6B) showed the same ANXA2 expression pattern as carcinogenic cells, in contrast with the loss of ANXA2 signal detected in the corresponding normal bile duct epithelium (Figure 2.6A). ANXA2 staining was preferably membranous in location (Figure 2.6D), although some cytoplasmic staining was observed (Figure 2.6C). IHC demonstrated that ANXA2 was frequently expressed in CCA. Biopsies from 227 patients (76.2%) stained positively for ANXA2. Increased expression of ANXA2 did not show a preference for any histological subtypes of tumor or tumor size. However, statistical analyses showed that positive staining for ANXA2 significantly associated with poor prognosis. High expression of ANXA2 was found to be associated with lymphatic invasion ($p = 0.014$), metastasis ($p = 0.026$) and perineural invasion ($p = 0.009$) (Table 2.2).

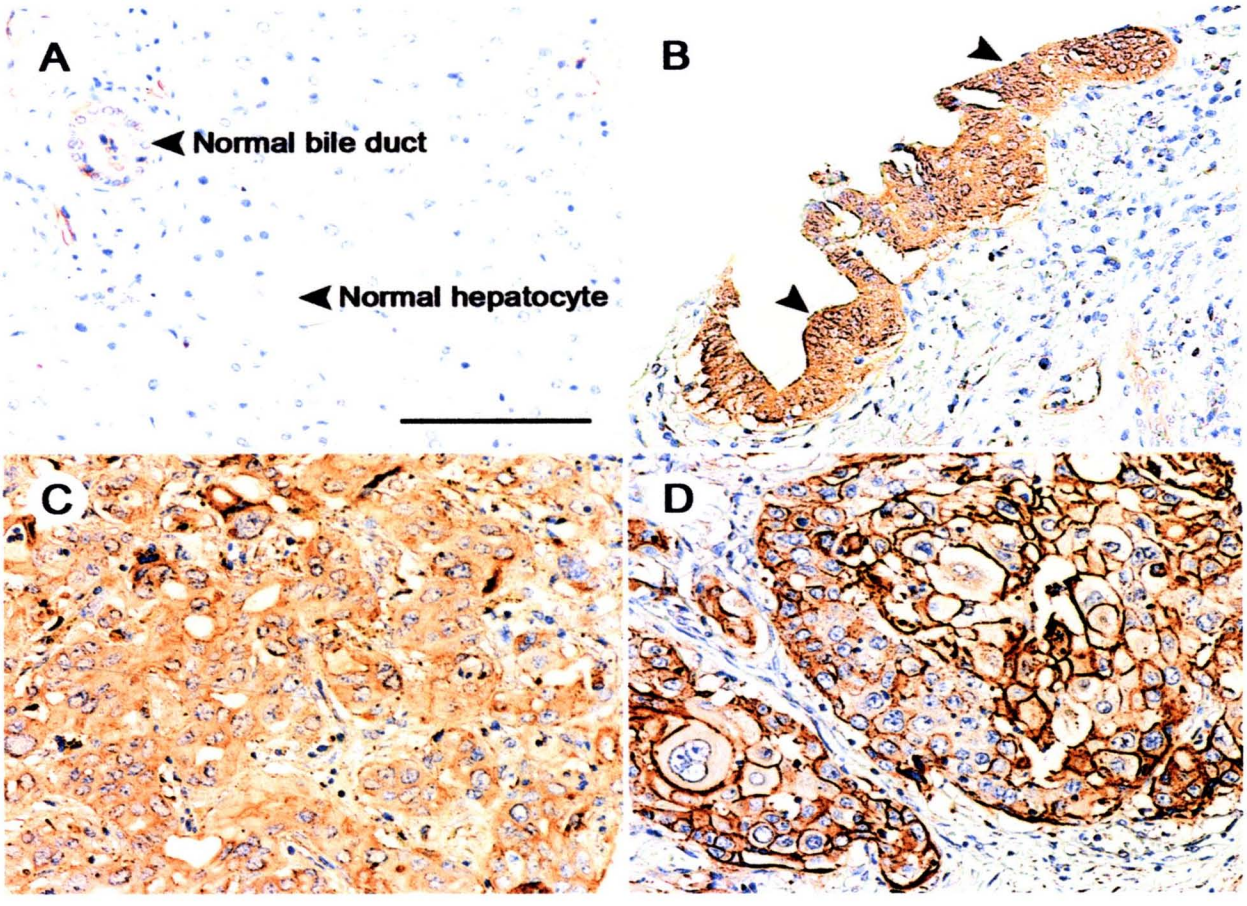

Figure 2.6 Immunohistochemical staining of Annexin A2 (ANXA2) in normal liver tissue (A), bile duct hyperplasia tissue (B) and cholangiocarcinoma (CCA) tissues (C and D). Annexin A2-positive cells were clustered within bile duct hyperplasia (B) and CCA tissues (C and D), but not detected or expressed at very low levels in stroma, normal liver and bile duct cells (A). Annexin A2 was preferably membranous (D) in location of CCA tissues, although some cytoplasmic staining (C) was observed. Immunoperoxidase staining, original magnification x200 (A-D); scale bar = 50 μm.

THE NATIONAL RESEARCH COUNCIL OF THAILAND
RESEARCH LIBRARY

Table 2.2 Clinicopathological variables and the expression status of annexin A2 (ANXA2) in *Opisthorchis viverrini*-induced cholangiocarcinoma tissues.

Variables	Annexin A2		*p*
	-ve	+ve	
Age(yr)			
≤ 56	50	114	0.001
> 56	19	111	
Gender			
Male	46	156	NS
Female	24	70	
Histotype group			
Less diff.	42	130	NS
Well diff.	19	76	
Gross type			
Mass forming	36	108	NS
Periductal infiltrating	11	49	
Intraductal	2	7	
Tumor size			
≤ 5 cm	28	87	NS
> 5 cm	27	59	
Vascular invasion			
Absent	34	100	NS
Present	32	118	
Lymphatic invasion			
Absent	25	49	0.014
Present	41	167	
Perineural invasion			
Absent	49	121	0.009
Present	17	94	
Metastasis			
Absent	36	92	0.026
Present	20	102	

Note: When the sum of subset numbers does not match patient totals, data were missing or unavailable. NS, not significant.

2.3.4 Expression of ANXA2 and cumulative survival

The median length of survival for patients with high ANXA2 expression was 27.42 weeks (95% Confidence Interval (95% CI), 22.26-32.58 weeks) whereas it was 42.86 weeks (95% CI, 25.92-59.80 weeks) for patients with low ANXA2 expression. Survival curves for the patients were generated based on the ANXA2 staining categories (Figure 2.7). Diminished survival was seen in the cases with high expression of ANXA2 (log-rank test, $p = 0.011$).

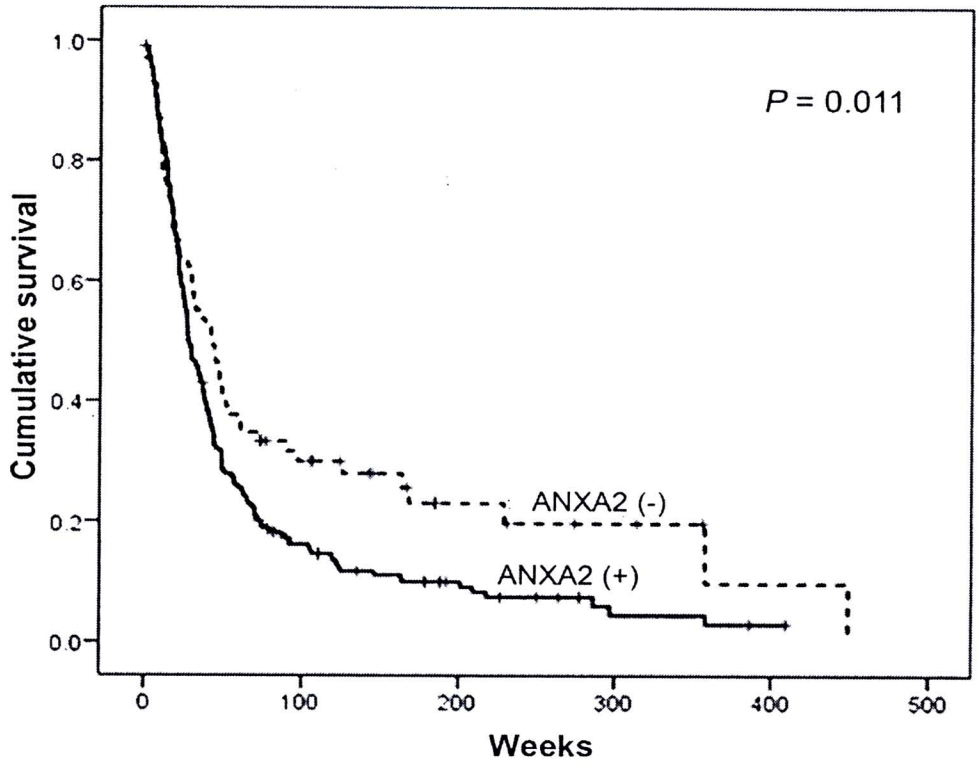

Figure 2.7 Survival curves using the Kaplan-Meier method. Significant unfavorable prognosis of cholangiocarcinoma (CCA) was high compared with low expression for annexin A2 (ANXA2) (*p = 0.011*). Annexin A2 (-) = low expression, annexin A2 (+) = high expression.

Ten potential prognostic factors were analyzed for their risk in the survival of *O. viverrini*-associated CCA (age, gender, histotype, gross type, tumor size, vascular invasion, lymphatic invasion, perineural invasion, metastasis, ANXA2 expression). In univariate analyses (log-rank test), vascular invasion (p = 0.003), lymphatic invasion (p = 0.001), metastasis (p = 0.001) and ANXA2 expression (p = 0.011) were found to be associated with survival time after surgery. Multivariate analysis (Cox-regression) was performed using the above four significant variables; lymphatic invasion (p = 0.001), metastasis (p = 0.003) and ANXA2 expression (p = 0.046) were identified as independent prognostic factors in *O. viverrini*-associated CCA (Table 2.3).

Table 2.3 Risk factors for overall survival in *Opisthorchis viverrini*-associated cholangiocarcinoma.

Risk factors	Overall survival				
	Univariate analysis (Log-rank)		Multivariate analysis (Cox regression)		
	Median time, wk	p	Relative risk	95%CI	p
Vascular invasion					
Absent	38.14 ± 3.06	0.003	0.78	0.61-1.00	NS
Present	25.42 ± 1.90		1		
Lymphatic invasion					
Absent	44.00 ± 4.82	0.001	0.59	0.43-0.81	0.001
Present	27.28 ± 1.95		1		
ANXA2					
Low expression	42.86 ± 8.64	0.011	0.71	0.51-0.99	0.046
High expression	27.42 ± 2.63		1		
Metastasis					
Absent	38.14 ± 4.57	0.001	0.65	0.49-0.86	0.003
Present	26.57 ± 2.65				

Note: CI, confident interval; NS, not significant.

2.4 Discussion

The complex biological fundamentals of CCA are still poorly elucidated, despite intensive studies. Several mechanisms by which *O. viverrini* infection may enhance cholangiocarcinogenesis have been proposed (Sripa et al., 2008). As in other epithelial neoplasms, it seems to develop through multiple processes involving DNA damage, deregulation of epithelial differentiation and abnormal cell proliferation (Sripa et al., 2008). With less apoptosis of the infected biliary epithelium, after several series of replication, genetic alterations may become fixed which can lead to neoplasm transformation (Sripa et al., 2007). Identification of the protein alterations associated with these events is important for understanding the mechanisms of cholangiocarcinogenesis and could facilitate the development of new tools for diagnosis, treatment and prevention of CCA.

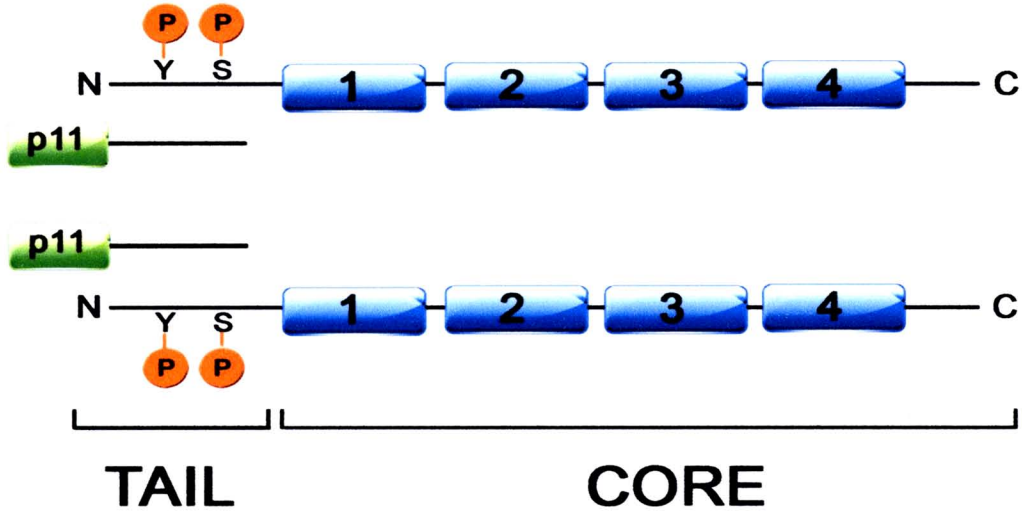

Figure 2.8 Structure of annexin A2 (ANXA2), shown as a heterotetramer with p11 (S100A10, light chain of 11 kDa). Similar to other family members, ANXA2 consist of a conserved "core" domain and a highly variable amino terminal tail domain. The four annexin repeats found within the core domain of the ANXA2 were represented as 1-4. The phosphorylation sites i.e., tyrosine and serine, are presented within the tail domain. Figure is adapted from Brownstein et al., 2001 (Brownstein et al., 2001).

Annexins are characterized by their capacity to bind to phospholipids in the presence of calcium ions and their susceptibility to phosphorylation and dephosphorylation (Rodrigo Tapia et al., 2007). Belonging to subfamily A of annexins of vertebrates, human annexins are further classified as annexin A1-A11 and A13 (Rodrigo Tapia et al., 2007). As shown in Figure 2.8, ANXA2 consists of a variable N-terminal "tail" domain that imparts specialized features to the molecule and a conserved C-terminal "core" domain that imparts phospholipid binding capacity (Yanay et al., 2001; Deora et al., 2004). ANXA2 has been shown to exist as a monomer, a heterodimer or a heterotetramer with S100A10 (light chain of 11 kDa, or p11) (Waisman, 1995). ANXA2 is located in the cell cytoplasm as a monomer (heavy chain of 36 kDa, or p36) or in a complex with a member of the S100A10 (Rodrigo Tapia et al., 2007). Heterotetramer formation between two copies of ANXA2 and two copies of S100A10 results in enhanced membrane phospholipid binding affinity (Erikson et al., 1980). Recent evidence indicates that ANXA2 is a constitutive regulator of the fibrinolytic process when located on the cell surface. ANXA2 serves as a receptor or binding protein for proteases (cathepsin B, plasminogen and tissue plasminogen activator or tPA) and proteins in the extracellular matrix (collagen and tenascin C) (Rodrigo Tapia et al., 2007). A relationship between proteases and extracellular matrix proteins through ANXA2 has been proposed whereby ANXA2 may facilitate the reorganisation of the extracellular matrix in physiological and pathological processes such as tumoral invasion (Mai et al., 2000). Based on this reason, the over-expression of ANXA2 has been verified in colorectal (Emoto et al., 2001b) and gastric (Emoto et al., 2001a) carcinomas, and was found to correlate with invasiveness and poor prognosis.

The expression of ANXA2 had already been described in tissues and cell lines of Korean ICC patients using expressed sequence tags (Wang et al., 2006), but there was a limited sample size which precluded IHC investigations (12 human ICC tissues and four normal liver tissues). Moreover, there are no data available on the expression of ANXA2 in *O. viverrini*-associated CCA which is commonly found in the northeast of Thailand.

In this study, we applied a proteomics-based approach to find differentially expressed tumor proteins in CCA cell lines. However, a drawback in using cell lines

is that the cells are not representative of the tissue of origin because they have been maintained and propagated in vitro for extended periods (Hay, 1988). Furthermore, each cell line was established from a few cells of a single patient biopsy, so cells may not accurately represent the tumor characteristics (Hay, 1988). Accordingly, validation of potential candidate tumor markers in patient biopsies is essential. ANXA2 was shown to be up-regulated in a proteomics study of cell lines among many other markers. Again, ANXA2 is known to play an important role in tumor invasion and metastasis in other cancers (Emoto et al., 2001a; Emoto et al., 2001b). Accordingly, ANXA2 was verified in human subjects by probing, using a commercial anti-mouse monoclonal antibody in the TMA of patients with CCA (301 diagnosed cases), where it was found to associate with one of several tumor progression stages as reflected by lymphatic invasion ($p = 0.014$) and metastasis ($p = 0.026$). In addition, the over-expression of ANXA2 found to be associated with decreasing perineural invasion in CCA tissues has been linked to tumoral suppression and the inhibition of cell migration as previously studied in other cancers (Liu et al., 2003; Rodrigo Tapia et al., 2007). A Cox-regression model was used in multifactorial analysis (age, gender, histotype, gross type, tumor size, vascular invasion, lymphatic invasion, perineural invasion, metastasis, ANXA2 expression and survival time after surgery), indicating ANXA2, vascular invasion, lymphatic invasion and metastasis had an association with survival time after surgery. As shown in Table 2.3, patients with low expression of ANXA2 had longer survival times after surgery compared with the patients with high expression of ANXA2, indicating that over-expression of ANXA2 may reflect tumor progression of *O. viverrini*-associated CCA. Regarding vascular invasion, lymphatic invasion and metastasis in our multifactorial analysis, it has been previously reported that the survival time after surgery for the group with the presence of tumor invasion and metastasis was shorter than the group with absence of tumor invasion and metastasis in CCA (Uttaravichien et al., 1999).

In conclusion, we have described, to our knowledge for the first time, that ANXA2 is expressed both in the cytoplasm and cell membrane of hyperplastic epithelia and CCA but not in normal cholangiocytes and hepatocytes. Our results indicate that up-regulated ANXA2 may serve as a prognostic marker for invasion, metastasis and survival in *O. viverrini*-associated CCA. We suggest that ANXA2 IHC

may be applied for diagnosis of CCA and prediction of patient outcome. Proteomic studies of tumor tissue and serum from patients with *O. viverrini*-associated CCA are of particular interest to aid the discovery of tumor markers and are currently underway in our laboratories.